Available online at www.sciencedirect.com
SCIENCE DIRECT®
Electrochemistry Communications 5 (2003) 549–554
electrochemistry communications
www.elsevier.com/locate/elecom

Structural change and capacity loss mechanism in orthorhombic Li/$LiFeO_2$ system during cycling

Y.S. Lee [a], S. Sato [b], M. Tabuchi [c], C.S. Yoon [d], Y.K. Sun [e], K. Kobayakawa [b], Y. Sato [b,*]

[a] *High-Tech Research Center, Kanagawa University, Yokohama 221-8686, Japan*
[b] *Department of Applied Chemistry, Kanagawa University, 3-27-1 Rokkakubashi, Yokohama 221-8686, Japan*
[c] *Special Division for Green Life Technology, National Institute of Advanced Industrial Science and Technology, 1-8-31, Midorigaoka, Ikeda, Osaka 563-8577, Japan*
[d] *Division of Material Science and Engineering, Hanyang University, Seoul 133-791, Republic of Korea*
[e] *Department of Chemical Engineering, Hanyang University, Seoul 133-791, Republic of Korea*

Received 8 May 2003; received in revised form 13 May 2003; accepted 13 May 2003
Published online: 29 May 2003

Abstract

Orthorhombic $LiFeO_2$ was synthesized at low temperature (150 °C) using a solid-state method. The Li/$LiFeO_2$ cell presented not only a high initial capacity of over 150 mAh/g, but also fairly good cycle retention of 73% after 50 cycles within a voltage range between 1.5 and 4.5 V. It was found that the orthorhombic phase of the $LiFeO_2$ material underwent a structural change to the spinel phase during cycling. Especially it showed severe structural changes during the first charge/discharge process, which might be the main reason to induce the capacity loss of the Li/$LiFeO_2$ system. We reported a new observation about the structural change mechanism of the orthorhombic Li/$LiFeO_2$ cell during cycling using in situ XRD and TEM analyses.

Keywords: Orthorhombic $LiFeO_2$; Magnetic property; Spinel $LiFe_5O_8$; Phase change

1. Introduction

Based on a number of studies for developing good cathode materials for lithium secondary batteries, many candidates have been intensively evaluated and considered from various view points, such as the cost, safety, and environmental aspects [1–18]. Although lithium iron oxide is the one of the strongest candidates to satisfy these considerations, it still shows some serious problems for use as a practical cathode material; such as a complex synthetic process and a lower operating voltage region [7–15]. Moreover, there has been no report that presents satisfactory cycling performance of the conventional $LiFeO_2$ (α-, β-, and γ-forms) which could be considered as a good cathode material for practical lithium secondary batteries.

Most recently, we have reported the synthesis of nanocrystalline orthorhombic $LiFeO_2$ material with advanced battery performance [19]. This material was successfully synthesized at low temperature (150 °C) using a solid-state method. The Li/$LiFeO_2$ cell at room temperature showed a high initial discharge capacity of over 150 mAh/g as well as a good cycle retention of over 73% after 50 cycles. Moreover, there are three new observations as follow: First, the unique role of pelletizing, which accelerated the slow reaction of lithium and the γ-FeOOH particles at a low synthesis temperature. Second, a Li/$LiFeO_2$ cell showed a unique capacity drop on the 13th cycle at the high current density of 0.4 mA/cm^2. Lastly, a Li/$LiFeO_2$ cell underwent a structural change from the orthorhombic to spinel phase during cycling, which was one main reason for the capacity loss during long-term cycling.

However, as mentioned in our previous report [19], there still remained some questions, such as the existence/role of the structural changes during the first cycle and the

* Corresponding author. Tel./Fax: +81-45-508-7480.
E-mail address: satouy01@kanagawa-u.ac.jp (Y. Sato).

1388-2481/03/$ - see front matter © 2003 Elsevier Science B.V. All rights reserved.
doi:10.1016/S1388-2481(03)00118-8

more critical investigation about the structural change in the Li/$LiFeO_2$ cell after long-term cycling. We report here the unique structural change of the orthorhombic $LiFeO_2$ material during the first cycle and suggest the capacity loss mechanism of the Li/$LiFeO_2$ cell during cycling.

2. Experimental

$LiFeO_2$ was synthesized using $LiOH \cdot H_2O$ (Kishida Chemical, Japan) and γ-FeOOH (High Purity Chemicals, Japan) by a conventional solid-state method. The stoichiometric amount of each material was ground and calcined at 150 °C for 15 h in an argon atmosphere in a box furnace.

The powder X-ray diffraction (XRD, Rint 1000, Rigaku, Japan) using Cu-Kα radiation was employed to identify the crystalline phase of the synthesized material. To investigate the structural change in the positive electrode during cycling, in situ XRD measurements were conducted using a homemade cell. Cell assembling and handling during the in situ XRD measurements were done in an argon-filled glove box to prevent any reaction with moisture in the air. After reaching the desirable voltage point, the in situ XRD cell was left in the glove box for 6 h to reach equilibrium during the entire measurement. To detect the spinel ferrites, a vibrational sample magnetometer (VSM, Riken Denshi, Japan) was used for collecting the magnetic field dependence of magnetization (*M–H*) data at 300 K. Magnetization curves were measured between −10 and +10 kOe. Additionally, the structural change in the $LiFeO_2$ electrode after cycling was observed using a transmission electron microscope (TEM, JEM 2010, JEOL, Japan) equipped with an energy-dispersive X-ray spectrometer (EDS) which was employed to characterize the microstructure of the electrodes after cycling.

The electrochemical characterizations were performed using coin-type cell. The cathode was fabricated with 20 mg of accurately weighed active material and 12 mg of conductive binder (8 mg of Teflonized acetylene black (TAB) and 4 mg of graphite). It was pressed on 200 mm^2 stainless steel mesh used as the current collector under a pressure of 300 kg/cm^2 and dried at 130 °C for 5 h in an oven. The test cell was made of a cathode and a lithium metal anode (Cyprus Foote Mineral Co.) separated by a porous polypropylene film (Celgard 3401). The electrolyte used was a mixture of 1 M $LiPF_6$–ethylene carbonate (EC)/dimethyl carbonate (DMC) (1:2 by vol, Ube Chemicals, Japan). The charge and discharge current density was 0.1 mA/cm^2 with a cut-off voltage of 1.5–4.5 V at room temperature.

3. Results and discussion

Fig. 1 shows the XRD pattern and cycle characterization of the orthorhombic $LiFeO_2$ material. The orthorhombic $LiFeO_2$ (herein referred to as o-$LiFeO_2$) was successfully synthesized using the LiOH and γ-FeOOH starting materials by a solid-state method at 150 °C under flowing argon. This XRD pattern and a TEM analysis from a previous report [19] revealed that this nano-crystalline $LiFeO_2$ consisted of well-crystallized orthorhombic $LiFeO_2$, spinel β-$LiFe_5O_8$, and defective $LiFeO_2$ phases. Fig. 1(b) shows the cycle characteristic of the Li/o-$LiFeO_2$ cell at room temperature. The test condition was a current density of 0.1 mA/cm^2 between 4.5 and 1.5 V. This o-$LiFeO_2$ electrode, which was tested at low current density in this study, showed no abrupt capacity loss which appeared on the 13th cycle at high current density (0.4 mA/cm^2) in the previous study. It shows a slightly increased discharge capacity up to the 3rd cycle and maintains a stable cycle performance between the 15th and 50th cycles. The absence of an abrupt capacity drop on the 13th cycle might have induced a different degree of lithium insertion/extraction due to the different current density during the charge/discharge process.

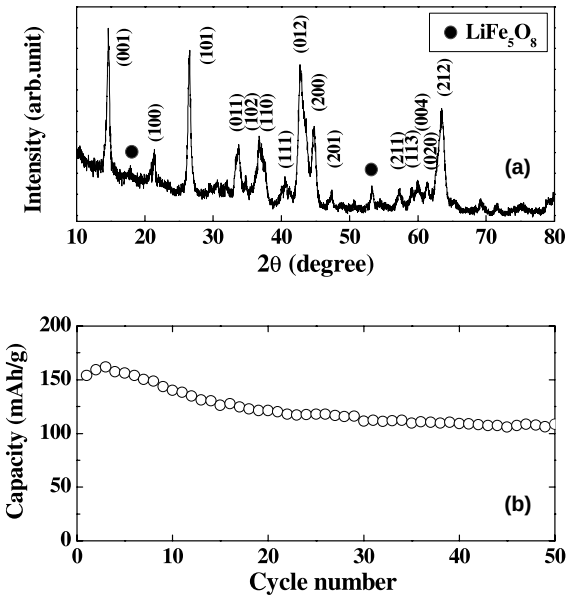

Fig. 1. (a) X-ray diffraction patterns of $LiFeO_2$, (b) cycle performance for the Li/1 M $LiPF_6$–EC /DMC/$LiFeO_2$ calcined at 150 °C for 15 h in argon. The test condition was a current density of 0.1 mA/cm^2 between 4.5 and 1.5 V at room temperature.

Fig. 2(a) show the charge/discharge curves of the Li/o-$LiFeO_2$ cell between the first and third cycles. After showing a long voltage plateau during the first charge process, the Li/o-$LiFeO_2$ cell showed a voltage drop at 3.0 V and three other long (or short) voltage plateaus during the first discharge process. The Li/$LiFeO_2$ cell seemed to occur many structural changes in the first discharge process. One of the more interesting observations is that this cell presents a fairly different cycle behavior from the second cycle as shown in Fig. 2(a).

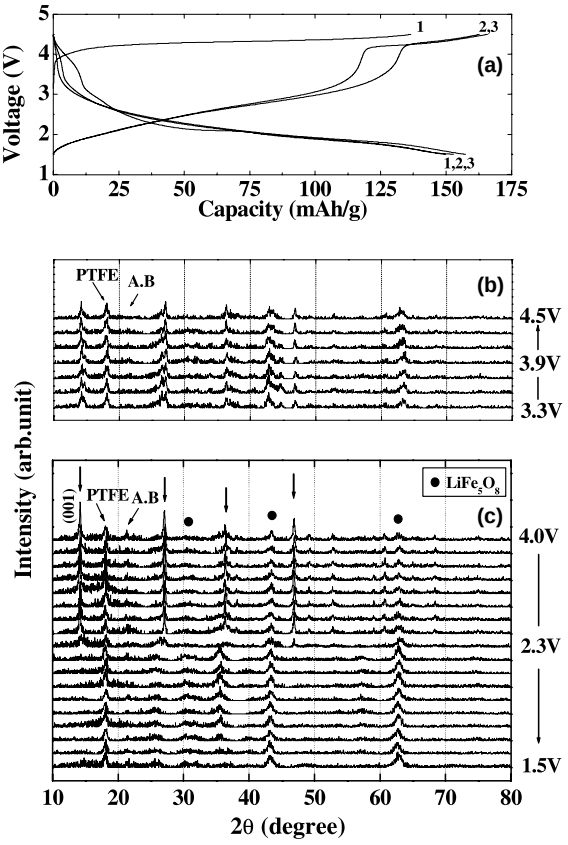

Fig. 2. (a) The charge/discharge curves and in situ XRD patterns for the Li/$LiFeO_2$ cell during (b) the first charge, and (c) the first discharge process.

To investigate the difference during the first cycle, in situ XRD of the Li/o-$LiFeO_2$ cell was conducted using a homemade in situ XRD cell. The counter and reference electrodes were prepared by pressing lithium foil onto stainless steel mesh. The cell construction of the in situ XRD cell was described in our previous report [20]. The test condition was the same as the cycling test at a current density of 0.1 mA/cm^2 between 4.5 and 1.5 V. Fig. 2(b) shows the in situ XRD patterns of Li/o-$LiFeO_2$ cell during the first charge process. As expected from the smooth voltage plateau in the charge curve, the in situ XRD during the first charge process showed no big difference in the whole XRD pattern, although some peaks are split into the two parts during charge and others peaks are slightly intensified according to the depth of charge. However, Fig. 2(c) shows clearly the many peak changes of the Li/o-$LiFeO_2$ cell during the first discharge process. The main orthorhombic peak at $2\theta = 14.6°$ was maintained to 2.4 V, however, it significantly decreased during the 2.3 V region and this clear (0 0 1) peak could not be detected any more after this point. Moreover, other major peaks also started to change in the 2.3 V region. Some of major peaks will diminish during deep lithium insertion into the Li_xFeO_2 structure, while the other small peaks of $2\theta = 43°$ or 63° (mainly spinel phase), in contrast to the strong major peaks, become the stronger peaks in the deep discharge state. Although it still failed to show the perfect spinel $LiFe_5O_8$ phase in this XRD diagram, the XRD pattern at 1.5 V is very similar to that of the spinel $LiFe_5O_8$ and starts to show the (2 2 0) peak of the $LiFe_5O_8$ spinel at $2\theta = 31°$ during the first discharge.

However, it still needs to define the real remained phase in/onto the electrodes after the first cycle, because some peaks in the XRD patterns after charge/discharge process are also partially similar to those of α and β-$LiFeO_2$ phases, such as (2 0 0) and (2 2 0) peaks of α-$LiFeO_2$. In order to confirm the remained phase in/onto the electrode after charge and discharge process, the magnetic properties of each sample (α-$LiFeO_2$, o-$LiFeO_2$, charged and discharged electrodes) were conducted using a VSM at room temperature. Because all conventional $LiFeO_2$ shows the antiferromagnetic ordering below room temperature, magnetic field (H) dependence of the magnetization (M) for the above samples successfully could detect a magnetic impurity like $LiFe_5O_8$ in/onto the powders and electrodes after charge and discharge process.

Fig. 3 shows the field dependence of the magnetization of various $LiFeO_2$ powders and electrodes. Unfortunately, α-$LiFeO_2$ powder in this study shows no ideal behavior in the M/H loop test, due to the small amount of impurity, which was obtained by hydrothermal method [12]. It is well known that this method is sometimes too difficult to obtain a single-phase compound, because it used many reaction steps and other chemicals during synthetic process. As described before,

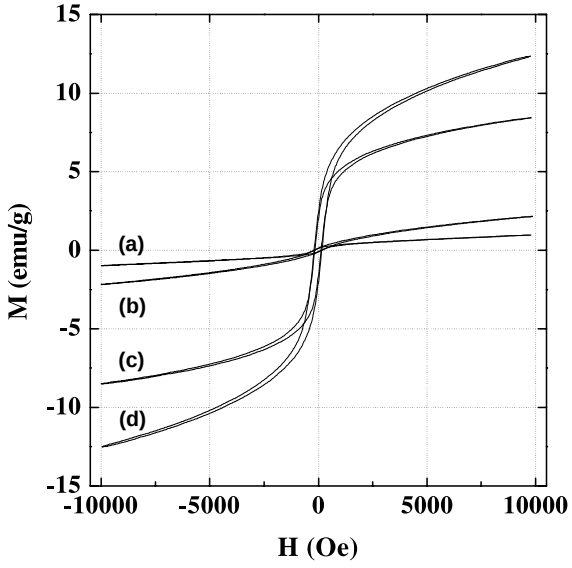

Fig. 3. Field dependence of the magnetization of various materials and electrodes. (a) Cubic α-$LiFeO_2$, (b) orthorhombic $LiFeO_2$, (c) the first charged state, and (d) the first cycled state of orthorhombic $LiFeO_2$ electrode.

orthorhombic $LiFeO_2$ material in this study was composed of an orthorhombic phase, a small amount of β-$LiFe_5O_8$, and defective $LiFeO_2$. The result of M–H test for orthorhombic $LiFeO_2$ powder showed a slightly shaped pattern due to the existed $LiFe_5O_8$ phase (about 1%) in the structure and the pattern of M/H curve was fairly similar to that of α-$LiFeO_2$ with a small amount of impurity. The weight fraction of β-$LiFe_5O_8$ ($M_s = 65$ emu/g at 300 K) in each sample was estimated as a ratio of the observed spontaneous magnetization, M_s (0.884(5) emu/g) to that of above magnetic impurity. The M_s value was calculated as an average one of extrapolated data at $H = 0$ from two least square lines consisted of M–H data more than 5 kOe or less than −5 kOe.

On the other hand, the electrodes after charge and discharge clearly reveal the structural change of Li/o-$LiFeO_2$ cell during the first cycling. In the case of the electrode after charge process, it clearly presents the S shape of conventional $LiFe_5O_8$ phase in the M–H test. The value of spontaneous magnetization of this electrode is 6.443(2) emu/g. Moreover, the electrode after the first cycle exhibits more developed S shape than that of one after the first charge. The value of magnetization for electrode after the first cycle is 8.68(2) emu/g. It means that the electrode after the first cycle has a larger amount of spinel $LiFe_5O_8$ phase than that of electrode after the first charge and it also explains clearly that the phase change, from the orthorhombic $LiFeO_2$ to the spinel $LiFe_5O_8$, is accelerated as the cycling proceeds. Based on these results, we could consider that the orthorhombic $LiFeO_2$ underwent severe structural changes during the first cycle, which induced a structural change from the orthorhombic to the spinel phase.

On the other hand, it also occurred to us how changed spinel phase could maintain (or develop) into the following cycles? In order to investigate the further structural change in the long-term cycling, $LiFeO_2$ electrodes in the discharged state after 3rd (the maximum point of discharge capacity) and 50th cycles were taken from the test cells in the glove box. The electrodes were washed with DMC solution to remove $LiPF_6$ salt and left in a glove box for 2 days to reach equilibrium after being tested from 1.5 to 4.5 V. Fig. 4 shows the TEM bright field image and electron diffraction patterns of the $LiFeO_2$ electrodes after the 3rd and 50th. As can be seen from the indexed polycrystalline ring pattern, nearly all of the initial o-$LiFeO_2$ phase was converted into the spinel phase after just the 3rd cycle as almost no trace of o-$LiFeO_2$ was observed using TEM analysis. A well-developed spinel structure was evidenced from the single crystal diffraction pattern in the [1 1 0] zone obtained from one of the particles in the cycled electrode. The diffraction pattern well matched that taken from the perfect spinel $LiFe_5O_8$ structure. After further cycling the electrode for 50 cycles, no significant structural changes were observed from the TEM analysis. Comparing the bright field images after the 3rd and 50th cycles, the particle size and morphology are quite similar, indicating that no further serious other structural transformations occurred after the first few cycles. The polycrystalline ring pattern and single crystal pattern in the [1 0 0] zone taken after 50 cycles also shows that the spinel structure was well maintained during the subsequent cycles after the initial structural transformation. The one difference between two electrodes, the electrode after 50 cycles occurred a large amount of defect and more serious phase transformation to the spinel phase,

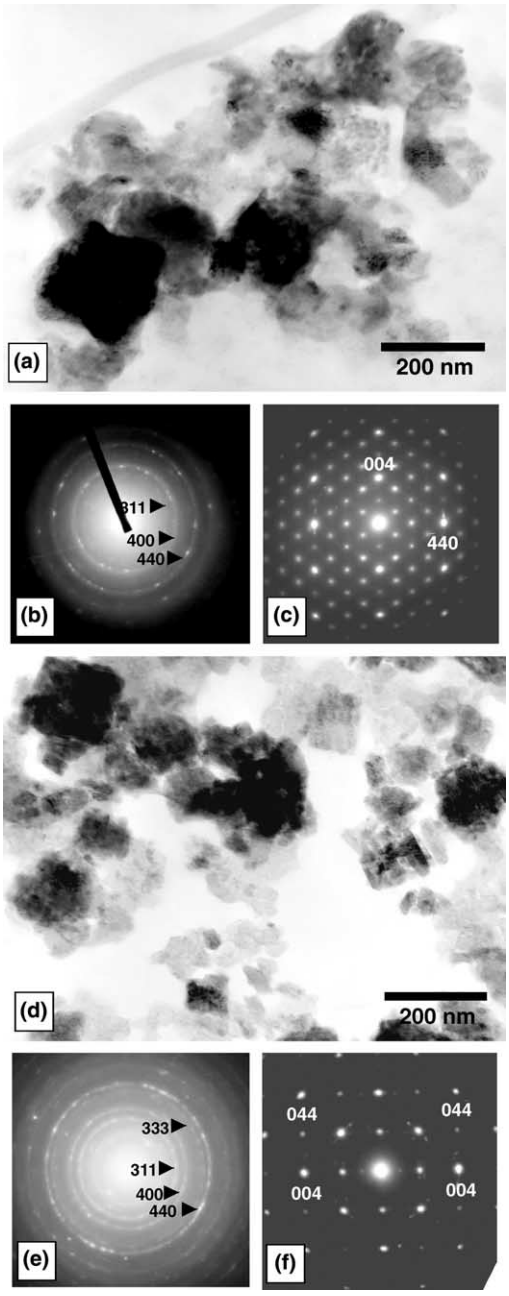

Fig. 4. TEM image and SAD patterns of electrodes after cycles (a–c) after the 3rd cycle, and (d–f) after the 50th cycle.

due to the long-term cycling. The TEM analysis conclusively proved that the phase transition from the orthorhombic structure to the spinel structure of the $LiFeO_2$ material was almost completed after the third cycle and that during the subsequent charge/discharge process, the electrode underwent a minimal structural change. Based on these results from the in situ XRD and TEM measurements, it could be considered that the orthorhombic Li/o-$LiFeO_2$ cell underwent severe structural changes into the spinel form during the early stage and continued transformation into the spinel $LiFe_5O_8$ phase during the long-term cycling. This indication was coincided with the result of ex situ XRD for Li/o-$LiFeO_2$ cells at various cycles in our previous report [19].

It is well known that the orthorhombic $LiMnO_2$ material exhibited a capacity loss during cycling, which is due to the conversion from the orthorhombic to spinel structure, although it showed increased discharge capacity in the early stage [5,6,18]. We also revealed the relation between the discharge curve and structural transformation of the Li/o-$LiMnO_2$ cell during cycling [21]. The discharge capacity of the Li/$LiMnO_2$ cell increased to the 10th cycle at high temperature (50 °C) accompanied by a spinel transformation. Moreover, the discharge curve at this point were very similar to that of the $LiMn_2O_4$ spinel, which could be easily confirmed by the change in the discharge curve during both the room and high temperature tests [21].

However, although these two materials have the same orthorhombic structure, we observed an interesting result that the Li/o-$LiFeO_2$ cell showed a severe phase change during the first cycle, although it also showed a small increase in the discharge capacity as in the Li/$LiMnO_2$ system during the early stage. The diagram of two materials regarding capacity loss during cycling is shown in Fig. 5. From the above results, conversely, we suspected that the poor cycle behavior of some $LiFeO_2$ materials in the previous reports, which showed abrupt capacity losses in the early stage, might result from the severe phase changes into the other structures in this stage [7,22].

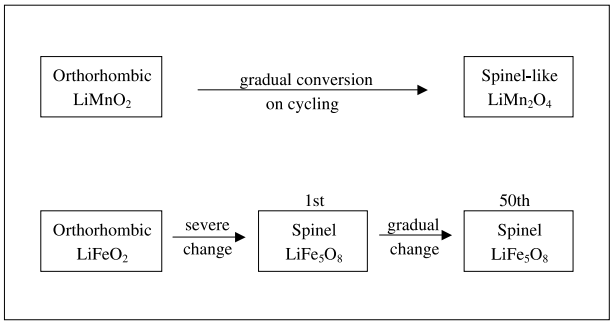

Fig. 5. Diagram of the capacity loss mechanism for the orthorhombic $LiMnO_2$ and $LiFeO_2$ materials.

4. Conclusion

Orthorhombic $LiFeO_2$ was synthesized at 150 °C using a solid-state method. The Li/$LiFeO_2$ cell presented not only a high initial capacity of over 150 mAh/g, but also a fairly good cycle retention of 73% after 50 cycles. We first found that the orthorhombic phase of the $LiFeO_2$ material underwent a structural change to the spinel phase during the first cycle and was maintained/developed into the well-formed spinel structure during the following cycle. A TEM analysis revealed that the clear spinel $LiFe_5O_8$ phase was found in the electrode after the 3rd cycle and there was no big difference compared with that of the electrode after 50 cycles. This means that the structural change into the spinel in the Li/o-$LiFeO_2$ cell was almost complete during the first cycle, which might be the main reason to induce the abrupt capacity loss of Li/o-$LiFeO_2$ cell during the early stage.

Acknowledgements

The authors gratefully acknowledge the financial support by the High-Tech Research Center Project from the Ministry of Education, Culture, Sports, Science and Technology.

References

[1] K. Mizushima, P.C. Jones, P.J. Wiseman, J.B. Goodenough, Mater. Res. Bull. 15 (1980) 783.
[2] J.R Dahn, U. Von Sacken, C.A. Michel, Solid State Ionics 44 (1990) 87.
[3] T. Ohzuku, A. Ueda, M. Nagayama, J. Electrochem. Soc. 140 (1993) 1862.
[4] H. Arai, S. Okada, Y. Sakurai, J. Yamaki, Solid State Ionics 95 (1997) 275.
[5] L. Croguennec, P. Deniard, R. Brec, A. Lecerf, J. Mater. Chem. 5 (1995) 1919.
[6] Y.I. Jang, B. Huang, H. Wang, D.R. Sadoway, Y.M. Chiang, J. Electrochem. Soc. 146 (1999) 3217.
[7] R. Kanno, T. Shirane, Y. Kawamoto, Y. Takeda, M. Takano, M. Ohashi, Y. Yamaguchi, J. Electrochem. Soc. 146 (1996) 2435.
[8] T. Shirane, R. Kanno, Y. Kawamoto, Y. Takeda, M. Takano, T. Kamiyama, F. Izumi, Solid State Ionics 79 (1995) 227.
[9] M. Tabuchi, K. Ado, H. Sakaebe, C. Masquelier, H. Kageyama, O. Nakamura, Solid State Ionics 79 (1995) 220.
[10] M. Tabuchi, C. Masquelier, T. Takeuchi, K. Ado, I. Matsubara, T. Shirane, R. Kanno, S. Tsutsui, S. Nasu, H. Sakaebe, O. Nakamura, Solid State Ionics 90 (1996) 129.
[11] K. Ado, M. Tabuchi, H. Kobayashi, H. Kageyama, O. Nakamura, Y. Inaba, R. Kanno, M. Takagi, Y. Takeda, J. Electrochem. Soc. 144 (1997) L177.
[12] M. Tabuchi, S. Tsutsui, C. Masquelier, R. Kanno, K. Ado, I. Matsubara, S. Nasu, H. Kageyama, J. Solid State Chem. 140 (1998) 159.
[13] M. Tabuchi, K. Ado, H. Kobayashi, I. Matsubara, H. Kageyama, M. Wakita, S. Tsutsui, S. Nasu, Y. Takeda, C. Masqulier, A. Hirano, R. Kanno, J. Solid State Chem. 141 (1998) 554.

[14] Y. Sakurai, H. Arai, S. Okada, J. Yamaki, J. Power Sources 68 (1997) 711.
[15] Y. Sakurai, H. Arai, J. Yamaki, Solid State Ionics 113–115 (1998) 29.
[16] T. Ohzuku, A. Ueda, T. Hirai, Chemistry Express 7 (1992) 193.
[17] J.N. Reimers, E.W. Fuller, E. Rossen, J.R. Dahn, J. Electrochem. Soc. 140 (1993) 3396.
[18] L. Croguennec, P. Deniard, R. Brec, J. Electrochem. Soc. 144 (1997) 3323.
[19] Y.S. Lee, C.S. Yoon, Y.K. Sun, K. Kobayakawa, Y. Sato, Electrochem. Commun. 4 (2002) 727.
[20] Y. Sato, T. Koyano, M. Mukai, K. Kobayakawa, Denki Kagaku 66 (12) (1998) 1215.
[21] Y.S. Lee, M. Yoshio, Electrochem. Solid-State Lett. 4 (10) (2001) A166.
[22] R. Kanno, T. Shirane, Y. Inaba, Y. Kawamoto, J. Power Sources 68 (1997) 145.